Clear Cell Sarcoma of the Kidney: Up-regulation of Neural Markers with Activation of the Sonic Hedgehog and Akt Pathways

Colleen Cutcliffe,[1] Donna Kersey,[1] Chiang-Ching Huang,[3] Yong Zeng,[3] David Walterhouse,[2] Elizabeth J. Perlman[1] for the Renal Tumor Committee of the Children's Oncology Group

Abstract **Purpose and Experimental Design:** Clear cell sarcoma of the kidney (CCSK), the second most common renal tumor in children, poses significant diagnostic challenges. No positive diagnostic markers are available, and the pathogenesis of CCSK remains an enigma. To address these challenges, the gene expression patterns of 14 CCSKs were compared with 15 Wilms tumors and 3 fetal kidney samples using oligonucleotide arrays.

Results: Using unsupervised methods, the gene expression profile of CCSK was distinctive: differentially expressed genes could largely be grouped into four categories: (*a*) a wide variety of neural markers, (*b*) members of the Sonic hedgehog pathway, (*c*) members of the phosphoinositide-3-kinase/Akt cell proliferation pathway, and (*d*) known therapeutic targets. Corresponding changes in critical proteins using Western blot and/or immunohistochemistry confirmed the up-regulation of these pathways and proteins. In particular, CD117 and epidermal growth factor receptor are up-regulated at the protein level in many CCSKs, providing potential therapeutic targets. One of the neural markers, nerve growth factor receptor, represents a promising diagnostic tool for CCSK.

Conclusions: This study suggests that CCSKs arise within a renal mesenchymal cell that shows a wide variety of neural markers. As such, it seems to be susceptible to genetic changes also seen in a variety of other neuroectodermal and neuronal tumors, including activation of Sonic hedgehog and phosphoinositide-3-kinase/Akt pathways. Involvement of these pathways in CCSKs implicates their widening role in tumorigenesis.

Clear cell sarcoma of the kidney (CCSK) arises most often in children <3 years of age and is the second most common renal tumor in children following Wilms tumor (1). Since its first description in 1970 (2), CCSK has presented significant diagnostic and clinical challenges. CCSKs are frequently misdiagnosed because they often resemble other pediatric renal tumors (3). During the last cooperative group clinical protocols, only 68% of CCSKs were correctly identified by the institutional pathologist. Currently, the diagnosis of CCSK is based solely on histologic features. Numerous studies have failed to identify immunohistochemical features or recurrent genetic changes that can reliably distinguish CCSKs from other pediatric renal tumors (1, 4). The accurate and timely diagnosis of CCSK is particularly critical because they are more aggressive than many other renal tumors, and they require chemotherapeutic regimens that include doxorubicin even at low stages (1, 5, 6). The identification of markers that distinguish CCSKs from other renal tumors could be used in conjunction with histology to improve the accuracy of diagnosis. Such markers would also shed light on the pathogenesis of CCSK, a tumor that is virtually exclusively found in the kidney and whose cell of origin remains an enigma. To address these questions, oligonucleotide microarrays were employed to compare the gene expression profiles of CCSK with those of Wilms tumor and fetal kidney samples. These studies show the genetic expression profile of CCSK to be highly distinctive. The finding that many of the genes up-regulated in CCSK are involved with neural differentiation, development, or function may be an important reflection of the cell of origin of CCSK. Additionally, two pathways activated in CCSK (Sonic hedgehog and phosphoinositide-3-kinase/Akt) have also been implicated in other pediatric neural tumors. Lastly, potential therapeutic targets are identified that may be useful in the treatment of CCSK.

Materials and Methods

Patient samples. Frozen tissue samples were obtained from the Renal Tumor Bank of the Children's Oncology Group. These were from unselected patients, and the pathologic diagnosis was provided by central pathology review. Samples were snap-frozen immediately following surgery and were mailed on dry ice to the Tumor Bank and

Authors' Affiliations: [1]Department of Pathology and Laboratory Medicine, [2]Division of Hematology/Oncology, Children's Memorial Hospital, and [3]The Department of Preventative Medicine, Northwestern University Feinberg School of Medicine, and the Robert H. Lurie Comprehensive Cancer Center, Chicago, Illinois
Received 6/22/05; revised 8/12/05; accepted 8/24/05.
Grant support: NIH U01 CA88131, U10 CA 42326, and U10CA98543.
The costs of publication of this article were defrayed in part by the payment of page charges. This article must therefore be hereby marked *advertisement* in accordance with 18 U.S.C. Section 1734 solely to indicate this fact.
Requests for reprints: Elizabeth J. Perlman, Children's Memorial Hospital, 2300 Children's Plaza, Box 17, Chicago, IL 60614. Phone: 773-880-4306; Fax: 773-880-3858; E-mail: eperlman@childrensmemorial.org.

doi:10.1158/1078-0432.CCR-05-1354

retained at −80°C. Studies were done with the approval of the Children's Memorial Hospital Institutional Review Board. Frozen sections were evaluated histologically prior to RNA isolation and tumors with <80% viable tumor cellularity were excluded. A total of 14 CCSKs, 15 blastemal Wilms tumor (three analyzed in duplicate), and 3 fetal kidneys (10, 15, and 16 weeks of gestation) were available for gene expression analysis.

RNA isolation. Total RNA was isolated from frozen tissues by Trizol (Invitrogen, Carlsbad, CA) extraction and treated with DNase I (Roche, Indianapolis, IN). No RNA amplification was done. The RNA was purified by RNeasy Mini Kit (Qiagen, Valencia, CA) and the concentration was determined by absorbance as measured by a GeneQuant DNA/RNA calculator (Amersham Biosciences, Piscataway, NJ). Samples with A_{260}/A_{280} of <1.8 were excluded. The quality of the RNA was further assessed by electrophoresis on a 1% agarose gel and samples rejected if significant RNA degradation was observed.

cDNA synthesis. cDNA synthesis was done by SuperScript Double-Stranded cDNA Synthesis Kit (Invitrogen). The manufacturer's protocol was modified by the use of a high-pressure liquid chromatography–purified T7-$(dT)_{24}$ primer (GenSet Oligos, Proligo, Boulder, CO) and incubation at 42°C rather than 37°C. The double-stranded cDNA product was purified by phenol/chloroform extraction using Phase Lock Gels (Eppendorf Scientific, Westbury, NY) followed by ethanol precipitation. The resulting pellet was washed twice in 80% ethanol, dried, and resuspended in 22 μL of RNase-free water.

Biotin-labeled cRNA synthesis. Twenty-two microliters of purified cDNA underwent an *in vitro* transcription using the BioArray High-Yield RNA Transcript Labeling Kit (Enzo, Farmingdale, NY). The resulting biotin-labeled cRNA was purified using RNeasy Mini Kit (Qiagen) and quantified using a GeneQuant DNA/RNA calculator (Amersham Biosciences). Samples were rejected from further analysis if the total yield from the *in vitro* transcription reaction was <30 μg per reaction. Labeled cRNA (17 μg) was fragmented according to the Affymetrix (Santa Clara, CA) protocol (http://www.affymetrix.com/support/technical/manual/expression_manual.affx).

Hybridization. The labeled, fragmented cRNA was added to a 300 μL volume of hybridization cocktail and hybridized to the Affymetrix HG-U133A oligonucleotide array (http://www.affymetrix.com/products/arrays/specific/hgu133.affx) for 16 hours at 45°C according to the Affymetrix protocol.

Washing, staining, and scanning. The hybridized microarrays were washed and stained using preprogrammed Affymetrix protocols. The arrays were stained with streptavidin-phycoerythrin (Molecular Probes, Eugene, OR) and the signal amplified using an antibody solution containing 0.1 mg/mL normal goat IgG (Sigma-Aldrich, St. Louis, MO), and 3 μg/mL biotinylated antistreptavidin antibody (Vector Laboratories, Burlingame, CA). The arrays were scanned in an HP GeneArray Scanner at the excitation wavelength of 488 nm. The amount of light emitted at 570 nm is proportional to the bound target at each location on the microarray.

Quality control. Following scanning, array images were assessed by eye to confirm scanner alignment and the absence of significant bubbles or scratches. The raw data (the cel files) can be found at http://www.ncbi.nlm.nih.gov/geo (accession number GSE2712). The digitalized image data were processed using Affymetrix GCOS software. Samples for which the 3′/5′ ratios for glyceraldehyde-3-phosphate dehydrogenase were >3.2 were excluded. The BioB spike controls were confirmed as present on 100% of the chips; BioC, BioD and cre were also present and in increasing intensity. When scaled to a target intensity of 2,500, scaling factors were between 12 and 53. Background (34-115), raw Q values (1.3-3.7), and mean intensities were within acceptable limits. The percentage of present calls ranged from 38% to 52%.

Statistical analysis. The data was first filtered to exclude genes which were "absent" in all samples and to exclude all Affymetrix control genes. The data was then normalized using a quantile-quantile normalization algorithm. For details of the quantile-quantile normalization algorithm, refer to http://dot.ped.med.umich.edu:2000/ourimage/microarrays/kerby_norm.htm. This resulted in the 15,666 probe sets used for the data analysis hereafter. The normalized data can be found in the Supplemental Data located at https://www.childrensmrc.org/CCSK_profile/. Hierarchical clustering was done using Spotfire software (Somerville, MA). To identify differentially expressed genes between CCSK and Wilms tumor, significance analysis of microarray was used (7). Principal component analysis was done on the standardized gene expression data (expression level for each gene has a mean of 0 and a SD of 1) by the method of singular value decomposition, and the first three principal components were plotted using the R statistical software (http://www.r-project.org).

Real-time quantitative RT-PCR. RNA from six CCSK samples and two fetal kidney samples were further analyzed by RT-PCR to confirm the RNA expression levels of five genes. The ABI Prism 7700 Sequence Detection System (Applied Biosystems, Foster City, CA) was used. Each 50 μL RT-PCR reaction (Applied Biosystems) volume included 25 ng of total RNA, 5 μL of TaqMan buffer A [500 mmol/L KCl, 100 mmol/L Tris-HCl, 0.1 mol/L EDTA, 600 nmol/L passive reference dye (pH 8.3) at room temperature], 10 μL of 25 mmol/L $MgCl_2$, 1.5 μL of each deoxynucleotide triphosphate (10 mmol/L dATP, dCTP, dGTP and 20 mmol/L dUTP), 0.5 μL of forward and reverse primers (10 μmol/L), 1 μL of corresponding TaqMan probe (5,000 nmol/L), 0.25 μL of AmpliTaq Gold supplied at 5 units/μL, and 0.25 μL MuLV reverse transcriptase. RT-PCR cycle variables were 48°C for 30 minutes, 95°C for 15 minutes, followed by 40 cycles at 95°C for 15 seconds, and 59°C for 1 minute. The primers and probes used in the study were designed using Primer Express software (Applied Biosystems). TaqMan probes, labeled with the reporter dye FAM and the quencher dye QSY7, and the actin primers used as a control were synthesized by Megabases, Inc. (Evanston, IL); the remaining primers were synthesized by Qiagen-Operon (San Francisco, CA). The probe sequences and primers are shown in Table 1. β-Actin was used as the endogenous control.

Immunohistochemistry. Paraffin-embedded tissue blocks were available for 10 CCSKs and 10 Wilms tumors. The following monoclonal antibodies were used: nerve growth factor receptor (NGFR; U.S. Biological, Swampscott, MA) at a dilution of 1:50, epidermal growth factor receptor (EGFR; DAKO Corp., Carpinteria, CA) at a dilution of 1:200, and CD117 (DAKO) at a dilution of 1:40. Following the appropriate secondary antibodies, the labeled antigens were visualized by a streptavidin-biotin system (Vectastain Elite ABC Kit, Vector Laboratories) followed by Vector NovaRed Substrate Kit (Vector Laboratories) and counterstained with hematoxylin (Richard-Allen Scientific, Kalamazoo, MI). Staining was quantified according to the following categories: strong staining of >50% of tumor cells, at least moderate staining of >20% of tumor cells, pale staining of <20% of tumor cells, and no staining.

Immunoblotting. Anti-AKT and anti-FKHR (FOXOA1) antibodies were purchased from Cell Signaling Technology (Beverly, MA), and anti-$GLI1_{803\text{-}818}$ antibodies from Rockland Immunochemicals for Research (Gilbertsville, PA). An antibody to β-actin (clone AC-15) from Sigma-Aldrich was used as a control to confirm equal loading. Protein lysates from six CCSKs and six Wilms tumors previously analyzed for gene expression were prepared by adding 500 μL sample buffer [0.125 mol/L Tris-HCl (pH, 6.8), 2% SDS, 10% glycerol, 0.001% bromophenol blue, and 5% β-mercaptoethanol] to 100 mg of frozen tissue followed by homogenization. DNA was sheared in a cold water bath sonicator for 40 minutes. 300 μg of total protein lysate was run on a 10% polyacrylamide SDS gel and transferred to a nitrocellulose membrane. The blots were rinsed then blocked with TBS containing 0.1% Tween 20 and 10% bovine serum albumin. Primary antibody was diluted in blocking buffer at a 1:1,000 dilution and incubated with the membrane overnight at 4°C. The blots were washed with either alkaline phosphatase antirabbit IgG (Vector Laboratories) for the GLI1, AKT, and FKHR (FOXOA1) antibodies, or alkaline phosphatase antimouse

Table 1. Primers and probes used for validation

Gene	TaqMan probe	Forward primer	Reverse primer
NPTX2	TGATGTTCCGCCCCACTGTGAAGAGT	CCATTAGAAGAAGGCTCCCATTT	CAGTGCTTACAAGAATCAACATGAATT
ECEL1	ACTGTCTACAACCAGCGGGTGAACGG	AGTGCATCGTCCGTCTCTATGAC	GTTCTCCCCAAGCGTGTGTT
LXH2	TGACTAGCCCCACCCTGCCAACTGT	GCCCACCACCCTGACAGA	TTGCCAGGCACAGAAGTTAAGA
NGFR	CATCCTGGCTGCTGTGGTTG	ACAACCTCATCCCTGTCTATTGCT	TGTTCCACCTCTTGAAGGCTATG
NTRK3	TGTTGGTGGTTCTCTTCGTCAT	CATCCTGGCTGCTGTGGTTG	TGGACCGTCGACCATATTTGT
ACTIN	ATGCCCTCCCCCATGCCATCCTGCGT	TCACCCACACTGTGCCCATCTACGA	CAGCGGAACCGCTCATTGCCAATGG

(Vector Laboratories) for the β-actin antibody. After washing, the color was developed with a 5-bromo-4-chloro-3-indolyl phosphate/nitroblue tetrazolium alkaline phosphatase substrate kit IV detection kit (Vector Laboratories).

Results

The gene expression profile of clear cell sarcoma of the kidney is distinctive when compared with Wilms tumor and fetal kidney samples. Gene expression analysis was done with 14 CCSKs, 15 Wilms tumors, and 3 normal fetal kidneys using Affymetrix HG-U133A chips (Affymetrix). Following normalization and filtering, 15,666 probe sets were included in the analysis. The data was first subjected to unsupervised hierarchical clustering as illustrated in Fig. 1A. The CCSKs clustered tightly together in a distinctly different group when compared with Wilms tumors and fetal kidneys. Three Wilms tumors were analyzed in replicate using RNA independently extracted on different days; these replicates clustered tightly together, providing confidence in the reproducibility of the data. To define genes that were significantly differentially expressed whereas reducing the number of false-positives, significance analysis of microarray was done and 413 probe sets corresponding to 330 genes were noted to be reliably differentially expressed. These can be found in the Supplemental Data (https://www.childrensmrc.org/perlman/). Over 20% of the genes detected were represented by more than one probe set, providing additional confirmation of, and confidence in, the genes involved. Principal component analysis is a multivariate method that reduces the high dimensionality of data to two or three viewable dimensions representing linear combinations of genes that account for most of the variance of the original data set. Principal component analysis was first applied to all 15,666 filtered probe sets (Fig. 1B) and then to the 330 genes selected by significance analysis of microarray (Fig. 1C). A distinct separation between Wilms tumor and CCSK was observed. The first principal component was able to separate Wilms tumor and CCSK completely.

To analyze the genes which were differentially expressed, the 330 genes selected by significance analysis of microarrays were analyzed by surveying the literature for known gene functions, and by investigating the biological pathways using Ingenuity Pathways Analysis software (Ingenuity Systems, Inc., Mountain View, CA). Twenty-two of the 330 genes are currently hypothetical. Many of the genes that were up-regulated in CCSKs could be grouped into four different but related categories: (*a*) genes involved in neural differentiation, neural expression, neural activity, and neural development (collectively referred to below as neural markers); (*b*) members of the Sonic hedgehog pathway; (*c*) members of the phosphoinositide-3-kinase/Akt pathway; and (*d*) potential therapeutic targets. Genes within the first three categories and their expression levels are listed and illustrated in Fig. 2. We further analyzed the genes overexpressed in each of these categories, paying special consideration to genes that function in more than one of these categories.

Up-regulation of neural markers. The largest group of genes up-regulated in CCSKs included genes involved in a wide variety of neural or neuronal activities, referred to collectively as neural markers. There were >30 genes belonging to this group, including neuronal pentraxins and their receptors, notch pathway genes, proto-oncogene *EGFR*, neurotrophins and their receptors, neural developmental genes, and neural growth factors (Fig. 2). To validate the gene expression data, a subset of these genes was analyzed by quantitative RT-PCR analysis, which confirmed the up-regulation of *NPTX2* (>15-fold), *LHX2* (>100-fold), *ECEL1* (>50-fold), *NGFR* (>18-fold), and *NTRK3* (>10-fold; Fig. 3). NGFR protein overexpression was confirmed by performing immunohistochemistry on archival sections of 10 different CCSKs and 10 Wilms tumors. All 10 CCSKs showed robust membranous staining with the NGFR antibody, with negative staining of adjacent renal elements (Fig. 4A). The 10 Wilms tumors (showing a spectrum of epithelial, blastemal, and stromal elements) were predominantly negative for NGFR using immunohistochemistry. In 2 of 10 cases, the paucicellular stroma separating the nodules of tumor was focally positive, and in a single case, small regions of undifferentiated stromal cells were strongly positive. To determine if NGFR staining could be of robust diagnostic utility, 11 congenital mesoblastic nephromas were similarly analyzed. These are mesenchymal tumors arising in young infants that are commonly mistaken for CCSK. Four classic congenital mesoblastic nephromas showed weak positivity of <25% of cells; one of five cellular congenital mesoblastic nephromas showed focal positivity. The majority of this tumor, and the remaining four tumors were entirely negative. Normal kidney showed the positivity of isolated cells in the distal tubules, the collecting ducts, and the urothelium, but the renal parenchyma was otherwise negative. In particular, a mesenchymal component expressing NGFR was not identified. These data suggest that NGFR is reliably and highly expressed in CCSKs at the RNA and protein levels, clearly differentiating them from Wilms tumors. The patchy positivity in other renal mesenchymal tumors, whereas distinctly different from the pattern shown in CCSKs, may limit its utility as a diagnostic immunohistochemical marker, although this merits further study in a larger group of tumors.

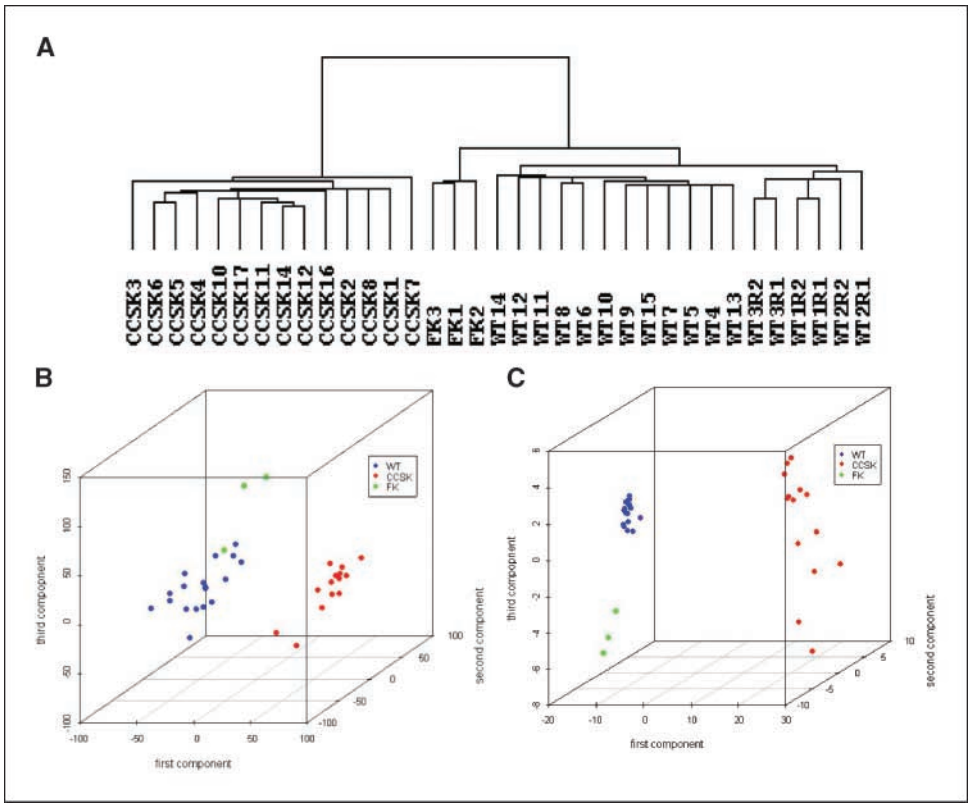

Fig. 1. Unsupervised analysis of 14 CCSK, 15 Wilms tumors, and 3 fetal kidney samples. *A,* hierarchical clustering using all 15,666 probe sets after filtering of the data set for probe sets that were absent across all samples. Three Wilms tumors were analyzed in replicate. *B,* principal component analysis using all 15,666 probe sets. *C,* principal component analysis using the 330 genes selected by significance analysis of microarray analysis.

Up-regulation of the Akt pathway. In addition to their roles in neural development, both NGFR and NTRK3 also function as receptors in the Akt pathway. This pathway regulates cell fate through inhibition of apoptosis, inhibition of necrosis, and promotion of cell proliferation (8). The hallmark gene of this pathway, *AKT1*, was among the 330 genes that were significantly up-regulated in CCSKs, and therefore, was targeted for additional analysis. Additional Akt pathway members that were up-regulated were *PIK3R1* (*p85*), *EGFR*, *NGFR*, *PTPNS1*, *GRB10*, *FOXO3A*, *FOXO1A*, *DAPK1*, *MAP3K5*, and *AR*. Further confirmation of activation of the Akt pathway was provided by the observation that the proapoptotic gene, *BNIP3L*, was down-regulated as illustrated in Fig. 2. The differential expression of *NGFR* and *NTRK3* was validated using quantitative RT-PCR as described above. To examine for corresponding protein up-regulation, we did Western blotting analysis using whole cell lysates from CCSKs and Wilms tumors and antibodies against Akt1, Foxo1a, and β-actin as control. The concentration of total Akt1 protein was equal among all six Wilms tumor samples and three of the CCSK samples tested. However, three CCSK samples exhibited an Akt1 concentration >2-fold higher compared with the Wilms tumor extracts (Fig. 4B). The full-length 69 kDa Foxo1a protein was detected at high levels in all six CCSK samples, but was almost undetectable in Wilms tumors (Fig. 4B). Western blots using antibodies against the phosphorylated Akt and/or Foxo1A were attempted, but phosphorylated protein was undetectable. This is not unexpected as these proteins are only briefly phosphorylated and the concentrations of phosphorylated Akt1 and Foxo1a are likely to be too low to be detected in these extracts. We conclude that the Akt pathway is likely to be up-regulated in CCSK compared with both Wilms tumor and normal fetal kidney based on the up-regulated expression of multiple genes in the pathway in addition to up-regulation of two hallmark proteins, Akt1 and Foxo1a.

Up-regulation of the Sonic hedgehog pathway. In addition to Akt pathway genes, a number of key genes in the Sonic hedgehog pathway were also up-regulated (Fig. 2). These include *PTCH* (the Sonic hedgehog receptor that is transcriptionally activated by GLI family transcription factors), and both *GLI1* and *GLI2* (transcription factors vital to Sonic hedgehog signaling; ref. 9). In addition, CCSKs show up-regulated expression of a variety of other Sonic hedgehog pathway genes, including *TWIST1* (a transcriptional activator of *GLI1*; ref. 10), *CCND1* (a promoter of cell proliferation; ref. 11), and *PDGFRA* and *PDGFA* (a growth factor/receptor duo; ref. 12). To explore the Sonic hedgehog pathway at the protein level, we did Western blot analysis of GLI1 on whole cell extracts from frozen CCSK and Wilms tumor samples. The 150 kDa, full-length GLI1 band was detectable in four of the six CCSK extracts, but was virtually undetectable in any of the six Wilms tumor extracts (Fig. 4B), indicating a potential role for the Sonic hedgehog pathway in the development of CCSKs.

Potential therapeutic targets. An important motivation for performing gene expression analysis of tumors is the potential to identify therapeutic gene targets. Several of the genes found to be up-regulated in CCSKs have already been targeted for inhibitor design and development. These include *AR*, *EGFR*, *KIT*, *NR3C1*, *PDE4A*, *PDGFRa*, and *PPP3Ca*. To further investigate and confirm these findings, 10 additional CCSKs were evaluated for expression of c-kit protein using antibodies directed against the CD117 and EGFR proteins (Fig. 4C). Of these 10 tumors, 1 showed strong membranous staining for CD117 in >50% of the tumor cells, 3 tumors showed at least moderate staining of

>20% of tumor cells, 2 tumors showed pale staining of <20% of cells, and 4 tumors were completely negative. For EGFR, 3 tumors showed strong membranous staining of >50% of the tumor cells, 1 tumor showed at least moderate staining of >20% of the tumor cells, 3 tumors showed pale staining of <20% of the tumor cells, and 3 were completely negative. Four of the 10 tumors showed <20% positivity for both markers.

Discussion

Among pediatric renal tumors, CCSKs are the most frequently misdiagnosed due to their histologic diversity, their rarity, and the lack of consistent immunohistochemical and genetic markers. Furthermore, little is known regarding the cell of origin or pathogenesis of CCSK. The goals of this study were (*a*) to identify markers that can accurately distinguish CCSKs, (*b*) to elucidate the pathways that are unique to CCSKs in order to gain a greater understanding of their pathogenesis, and (*c*) to identify potential therapeutic targets.

Potential neural cell of origin for clear cell sarcoma of the kidney. The largest category of genes up-regulated in CCSKs were neural markers, including genes involved in neural development, function, and differentiation. Some genes identified as up-regulated in CCSKs have also been shown to be

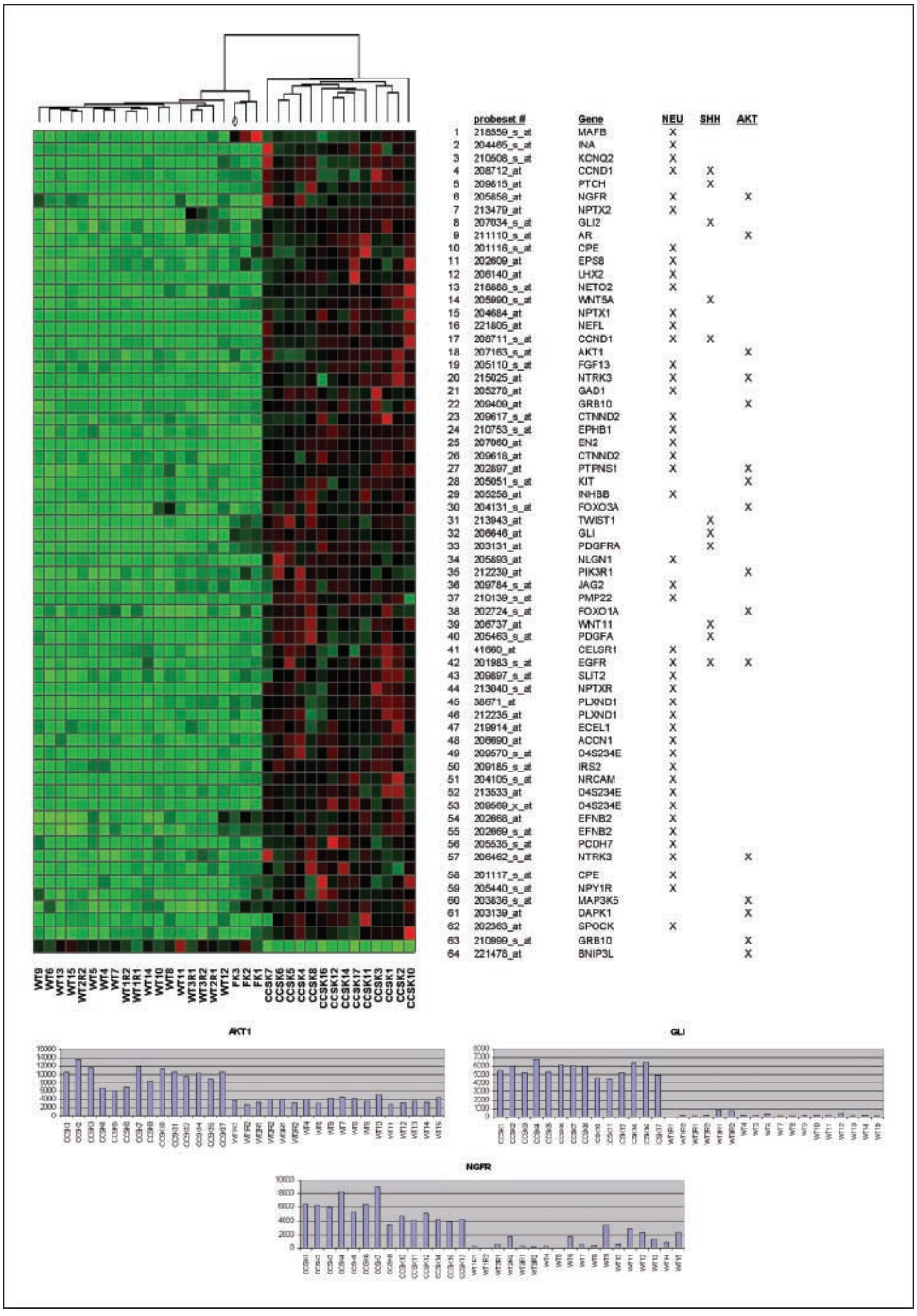

Fig. 2. Differential expression of neuronal, Sonic hedgehog, and Akt pathway genes in CCSK versus Wilms tumor. Genes shown were selected based on categorization to neural (*NEU*), Sonic hedgehog (*SHH*), or Akt pathways. Green, relative decrease in expression; red, relative increase in expression. The normalized expression levels for all tumors analyzed are shown for *AKT1* (Akt), *GLI* (Sonic hedgehog), and *NGFR*.

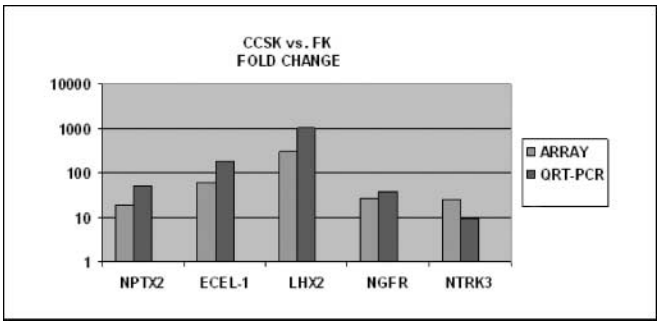

Fig. 3. Fold-change increase of genes validated by quantitative RT-PCR. RNA from six CCSK samples and two fetal kidney samples examined by microarray were further analyzed by quantitative RT-PCR to confirm RNA expression levels of five genes. β-Actin was used as the endogenous control. For every gene analyzed, the RT-PCR quantification resulted in similar fold change.

up-regulated in medulloblastomas as well as central and peripheral primitive neuroectodermal tumors (13–17). The most highly up-regulated gene in CCSKs was *LHX2*, a LIM homeodomain gene highly expressed in the developing brain, which showed >1,000-fold higher expression in CCSKs compared with Wilms tumors. Of particular interest was the up-regulation of two neurotrophin receptor genes: *NGFR* and *NTRK3* (*TRKC*). Both are known to be important determinants of cell death or survival (8, 18–20). Furthermore, both have been shown to be overexpressed in medulloblastomas (13, 14, 21). NGFR is a receptor for neurotrophins and is required for neuronal survival (19). Its ligand, nerve growth factor, binds and activates Trk tyrosine kinase receptors (15). The binding of nerve growth factor to NGFR stimulates signaling pathways that result in cell survival by reducing apoptosis. *NTRK3* and its receptor *NT3* were also up-regulated in CCSKs.

The up-regulation of neural genes in CCSK may provide insight into the cell of origin of this elusive tumor. The fact that CCSKs are virtually exclusively found in the kidney of infants suggests that CCSKs arise within a mesenchymal cell of the developing kidney during gestation. If this hypothesis is correct, then there are three alternatives: (*a*) CCSKs may arise in a neural progenitor cell misplaced during development, (*b*) a renal mesenchymal cell may develop aberrant neural markers early in tumor development, or (*c*) CCSK may arise in a primitive mesenchymal cell in the kidney that shows neural markers for a restricted period of time during development. Both NGFR and NTRK3 have been shown to be expressed in the developing human kidney. *In situ* hybridization and immunohistochemical analyses show expression predominantly in the developing epithelial components of the kidney rather than the mesenchyme. However, NGFR expression has been noted to be present in the perivascular mesenchymal tissue in 19-week-old human fetuses, but not in full-term fetuses (22). This supports the hypothesis that CCSKs (tumors characterized by a proliferation

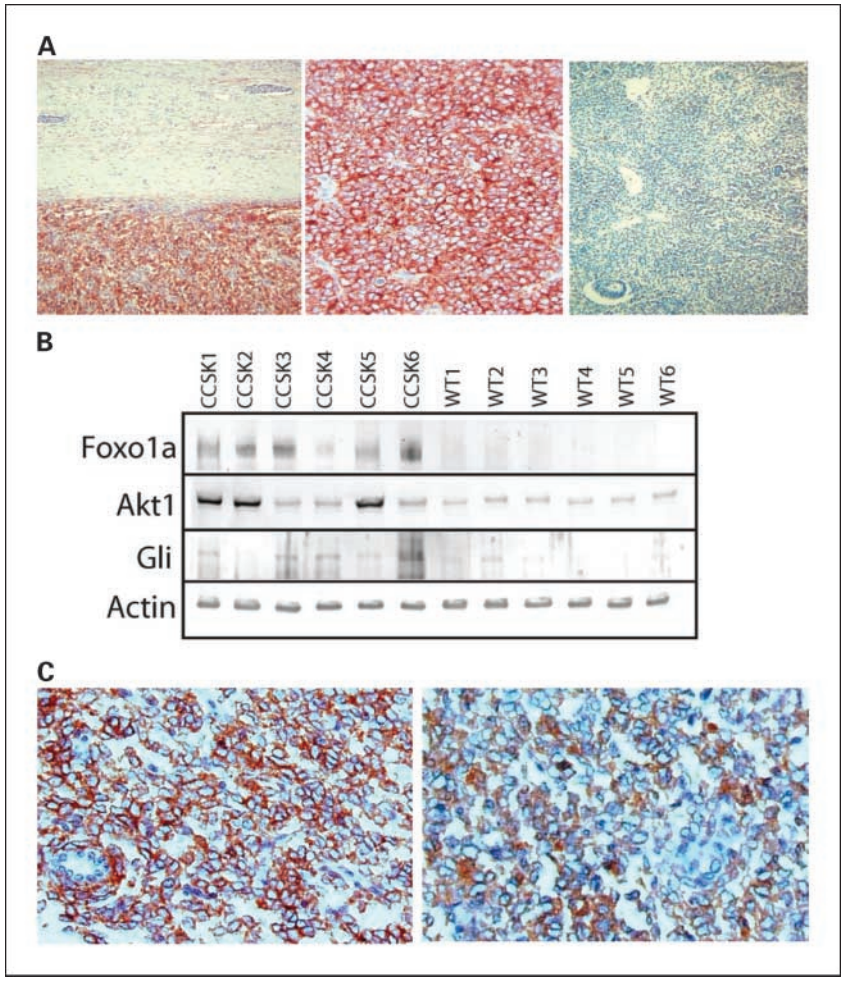

Fig. 4. Validation of protein expression of up-regulated genes in CCSK. *A,* formalin-fixed, paraffin-embedded histologic sections of 10 Wilms tumor and 10 CCSKs were analyzed by immunohistochemical methods using antibody to NGFR. All of the CCSKs (*left, middle*) had robust membrane staining and negative staining in the stroma of the example shown (*left*). All Wilms tumors were negative (*right*). *B,* Western blotting analysis of six CCSKs and six Wilms tumors with antibody against Akt1, Foxo1a, Gli1, and the β-actin control. Lanes 1 to 6 are CCSK extracts, whereas lanes 7 to 12 are Wilms tumor extracts. *C,* formalin-fixed, paraffin-embedded histologic sections of 10 CCSKs were analyzed by immunohistochemistry using antibodies to CD117 (*right*) and EGFR (*left*). CCSKs demonstrated strong staining of >50% of tumor cells.

of mesenchymal cells surrounding a unique fine vascular network) may arise from such mesenchymal cells during a confined period of development when they express *NGFR*.

The up-regulation of neural markers in CCSK also promises to provide diagnostic tools for this lesion that is frequently misdiagnosed due to the current lack of positive diagnostic markers. The most promising marker in our study is NGFR, which was strongly and reliably up-regulated in all CCSKs using immunohistochemistry, a tool available in all histology laboratories. This will need to be formally analyzed within a larger cohort of CCSKs as well as a diversity of other tumors arising in the pediatric kidney.

Activation of the AKT pathway in clear cell sarcoma of the kidney. One of the signaling pathways activated by NGFR and NTRK3 is the Akt cell proliferation pathway, illustrated in Fig. 5A. Overall, activation of Akt results in increased cell proliferation and concurrent inhibition of apoptosis and necrosis (23). The Akt pathway becomes activated by signaling from a variety of receptors, including NGFR, EGFR (24), and *NTRK3* (15), which were all found to be up-regulated in CCSKs. These tyrosine kinase receptors become phosphorylated upon growth factor binding, and the phosphorylated receptor recruits the p85/p110 complex. In addition to *p85*, *GRB10* was also up-regulated: GRB10 associates with p85 and activates the Akt pathway through an unknown mechanism (25, 26). The p85/p110 complex catalyzes activity that results in the recruitment of AKT1 to the plasma membrane, where it becomes activated by phosphorylation. Subsequent to phosphorylation of Akt1, a variety of signal transduction pathways become activated, resulting in the activation and/or repression of a wide variety of genes. Among the outcomes of Akt activation is the phosphorylation of forkhead transcription factors *FOXO1A* and *FOXO3A*, resulting in their inactivation. The forkhead transcription factors function to up-regulate genes involved in necrosis, apoptosis, and cell cycle arrest. The ultimate consequence of their inactivation is an increase in cell survival and proliferation (23, 27). Genes for two key forkhead proteins, *FOXO1A* and *FOXO3A*, were up-regulated in CCSKs. One target of *FOXO3A* that promotes apoptosis is *BNIP3L*. Further compelling evidence of the deactivation of forkhead transcription factors, and hence activation of the Akt pathway, is the down-regulation of *BNIP3L* seen in CCSKs (28). Another direct target of AKT1 shown to be up-regulated in CCSKs is *MAP3K*, which results in increased cellular proliferation via the mitogen-activated protein kinase pathway. We identified up-regulation of total Akt1 protein in half of the CCSKs tested. Because the active form of Akt is phosphorylated, it is possible that the tumors which did not show up-regulated overall Akt may contain up-regulated phosphorylated Akt1. Akt pathway components are frequently altered in human cancers, and may also be involved in drug resistance. Furthermore, efforts are under way to develop treatment strategies that target these specific signaling molecules and their downstream effectors (23).

Activation of the Sonic hedgehog pathway in clear cell sarcoma of the kidney. This study shows up-regulation of *PTCH* and *GLI1* in addition to many other genes known to act within the Sonic hedgehog pathway (*GLI2*, *CCND1*, *PDGFA*, *PDGFRA*, and *TWIST1*; refs. 10, 29–31). The Sonic hedgehog signaling pathway governs patterns of cell growth and differentiation in a wide variety of embryonic tissues, and is illustrated in Fig. 5B. The receptor of the Sonic hedgehog ligand (Shh) is Patched (Ptch), which normally functions to restrain the activity of Smoothened (Smo; ref. 32). When Shh binds with Ptch and the pathway is activated, Smo is unrestrained and is allowed to initiate a signaling cascade that results in nuclear translocation of the GLI transcriptional activators which are the primary regulators of the downstream targets of the Sonic hedgehog pathway (33, 34). The transcription of *PTCH* is also induced by Sonic hedgehog activity, generating a negative feedback loop and serving as a convenient indicator of Sonic hedgehog pathway activation (35). Activation of the Sonic hedgehog pathway has been linked to several types of human tumors. The most direct example is Gorlin syndrome, an autosomal dominant disorder associated with heterozygous loss-of-function mutation in *PTCH*. Patients with Gorlin syndrome have increased incidence of many tumors, most notably basal cell carcinoma, medulloblastoma, rhabdomyosarcoma, and fibrosarcomas. Similar mutations in *PTCH* or activating mutations in *SMO* are found in 40% of sporadic basal cell carcinomas, 25% of primitive neuroectodermal tumors (24), and in a histologic subtype of medulloblastomas (14, 36). Small cell carcinomas of the lung, on the other hand, lack *PTCH* and *SMO* mutations, and in these tumors, Sonic hedgehog pathway activity is proposed to be secondary to endogenous overexpression of Sonic hedgehog ligand. Further studies are necessary to identify the underlying cause of the pathway activation in CCSKs, including analysis for *SMO* and *PTCH* mutations. Of therapeutic interest, a plant steroidal alkaloid, cyclopamine, binds to and inactivates SMO. Treatment with cyclopamine dramatically reduces pathway activity in cells driven by Sonic hedgehog activation, whether due to mutations or endogenous overexpression (37).

Potential therapeutic targets. Potential therapeutic targets identified as up-regulated in CCSK included EGFR, KIT, and PDGFRα. These represent only part of a larger ongoing identification of tyrosine kinases in multiple cancer types. The goal is to provide orally administrable, safer methods of treatment than the current chemotherapeutic agents used. Thus far, several of these identified inhibitors have proved highly successful in a variety of tumor types. The most well characterized, gefitinib, has been targeted to patients exhibiting >10% EGFR positive staining by immunohistochemistry. This treatment has been reported to be effective in non–small cell lung, prostate, head and neck, colorectal, and ovarian cancers [reviewed in Vlahovic et al. (38)]. Our data suggest that up to 70% of CCSKs may show >10% EGFR staining. Similarly, gastrointestinal stromal tumors have been shown to contain either KIT mutation (resulting in overexpression of CD117) or PDGFRα mutation. Patients with gastrointestinal stromal tumors who have either of these mutations are often responsive to imatinib mesylate (STI571), another tyrosine kinase inhibitor (reviewed in ref. 39). This inhibitor has also been shown to be effective in treating dermatofibrosarcoma protuberans, giant cell fibroblastoma, and glioblastoma (40, 41). Our study suggests that at least 40% of CCSKs may show expression of CD117 at levels that correlate with inhibitor effectiveness in other tumor systems. In conclusion, one or more of the currently known tyrosine kinase inhibitors might be effective in the treatment of CCSKs. Future studies will rely on the creation of tissue microarrays representing tumors of patients registered in the Children's Oncology Group protocols and examining the relationship between EGFR

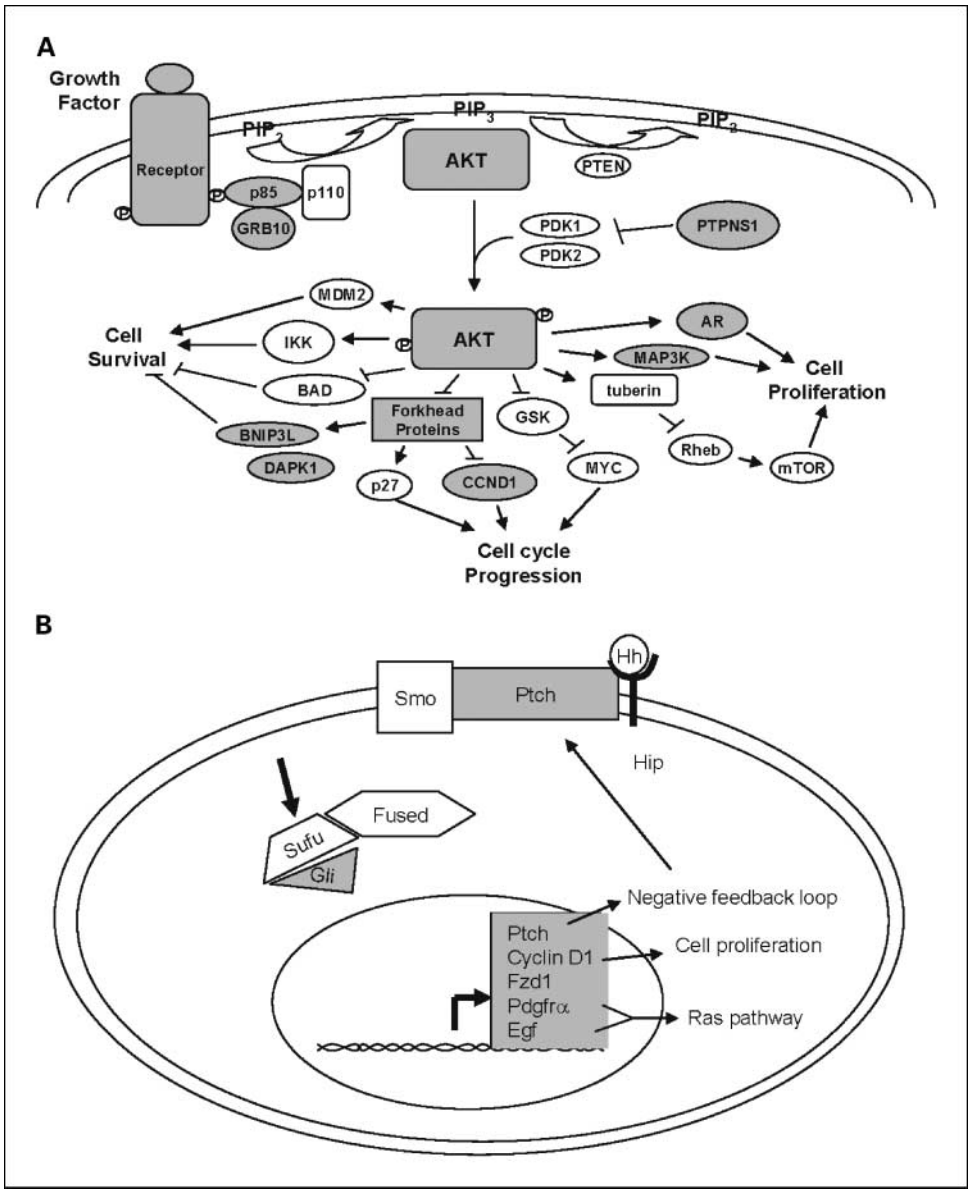

Fig. 5. *A,* schematic diagram of the Akt pathway. *B,* schematic diagram of the Sonic hedgehog pathway: the proteins that are shaded are among those encoded by the 330 differentially expressed genes detected by gene expression analysis in this study.

and KIT expression, as well as the other up-regulated therapeutic targets, with clinical variables including stage, relapse, and responsiveness to therapy. In addition, genetic studies need to be done to assess whether or not mechanisms that have been shown to result in overexpression in other tumors (such as activating mutations) are also in play with CCSK.

Acknowledgments

The authors acknowledge the effort and support of pathologists, oncologists, radiologists, and clinical research assistants who have contributed the significant efforts required to develop the unique clinical resources comprising the National Wilms Tumor Study Group-5, led by Drs. Daniel Green and Paul Grundy.

References

1. Argani P, Perlman EJ, Breslow NE, et al. Clear cell sarcoma of the kidney: a review of 351 cases from the National Wilms Tumor Study Group Pathology Center. Am J Surg Pathol 2000;24:4–18.
2. Kidd JM. Exclusion of certain renal neoplasms from the category of Wilms tumor. Am J Pathol 1970; 58:16a.
3. Beckwith JB. Renal neoplasms of childhood. 2nd ed. In: Sternberg SS, editor. Diagnostic surgical pathology. New York: Raven Press; 1994. p. 1741–66.
4. Schuster AE, Schneider DT, Fritsch MK, Grundy P, Perlman EJ. Genetic and genetic expression analyses of clear cell sarcoma of the kidney. Lab Invest 2003; 83:1293–9.
5. Beckwith JB. Wilms' tumor and other renal tumors of childhood. Major Probl Pathol 1986;18:313–32.
6. Seibel NL, Li S, Breslow NE, et al. Effect of duration of treatment on treatment outcome for patients with clear-cell sarcoma of the kidney: a report from the National Wilms' Tumor Study Group. J Clin Oncol 2004;22:468–73.
7. Tusher VG, Tibshirani R, Chu G. Significance analysis of microarrays applied to the ionizing radiation response. Proc Natl Acad Sci U S A 2001;98:5116–21.
8. Barnabe-Heider F, Miller FD. Endogenously produced neurotrophins regulate survival and differentiation of cortical progenitors via distinct signaling pathways. J Neurosci 2003;23:5149–60.
9. Villavicencio EH, Walterhouse DO, Iannaccone PM. The Sonic hedgehog-patched-Gli pathway in human development and disease. Am J Hum Genet 2000;67: 1047–54.
10. Villavicencio EH, Yoon JW, Frank DJ, Fuchtbauer EM, Walterhouse DO, Iannaccone PM. Cooperative E-box regulation of human GLI1 by TWIST and USF. Genesis 2002;32:247–58.

11. Louro ID, Bailey EC, Li X, et al. Comparative gene expression profile analysis of GLI and c-MYC in an epithelial model of malignant transformation. Cancer Res 2002;62:5867–73.

12. Xie J, Aszterbaum M, Zhang X, et al. A role of PDGFRα in basal cell carcinoma proliferation. Proc Natl Acad Sci U S A 2001;98:9255–9.

13. Keles GE, Berger MS, Schofield D, Bothwell M. Nerve growth factor receptor expression in medulloblastomas and the potential role of nerve growth factor as a differentiating agent in medulloblastoma cell lines. Neurosurgery 1993;32:274–80.

14. Pomeroy SL, Tamayo P, Gaasenbeek M, et al. Prediction of central nervous system embryonal tumour outcome based on gene expression. Nature 2002;415:436–42.

15. Ivanisevic L, Banerjee K, Saragovi HU. Differential cross-regulation of TrkA and TrkC tyrosine kinase receptors with p75. Oncogene 2003;22:5677–85.

16. Yoon JW, Kita Y, Frank DJ, et al. Gene expression profiling leads to identification of GLI1-binding elements in target genes and a role for multiple downstream pathways in GLI1-induced cell transformation. J Biol Chem 2002;277:5548–55.

17. Chiappa SA, Chin LS, Zurawel RH, Raffel C. Neurotrophins and Trk receptors in primitive neuroectodermal tumor cell lines. Neurosurgery 1999;45:1148–54.

18. Denkins Y, Reiland J, Roy M, et al. Brain metastases in melanoma: roles of neurotrophins. Neuro-oncol 2004;6:154–65.

19. Kirstein M, Farinas I. Sensing life: regulation of sensory neuron survival by neurotrophins. Cell Mol Life Sci 2002;59:1787–802.

20. Casaccia-Bonnefil P, Gu C, Chao MV. Neurotrophins in cell survival/death decisions. Adv Exp Med Biol 1999;468:275–82.

21. Kokunai T, Sawa H, Tamaki N. Functional analysis of trk proto-oncogene product in medulloblastoma cells. Neurol Med Chir (Tokyo) 1996;36:796–804.

22. Huber LJ, Hempstead B, Donovan MJ. Neurotrophin and neurotrophin receptors in human fetal kidney. Dev Biol 1996;179:369–81.

23. Fresno Vara JA, Casado E, de Castro J, Cejas P, Belda-Iniesta C, Gonzalez-Baron M. PI3K/Akt signalling pathway and cancer. Cancer Treat Rev 2004;30:193–204.

24. McKenna WG, Muschel RJ, Gupta AK, Hahn SM, Bernhard EJ. The RAS signal transduction pathway and its role in radiation sensitivity. Oncogene 2003;22:5866–75.

25. Deng Y, Bhattacharya S, Swamy OR, et al. Growth factor receptor-binding protein 10 (Grb10) as a partner of phosphatidylinositol 3-kinase in metabolic insulin action. J Biol Chem 2003;278:39311–22.

26. Ichihara M, Murakumo Y, Takahashi M. RET and neuroendocrine tumors. Cancer Lett 2004;204:197–211.

27. Blume-Jensen P, Hunter T. Oncogenic kinase signalling. Nature 2001;411:355–65.

28. Unoki M, Nakamura Y. EGR2 induces apoptosis in various cancer cell lines by direct transactivation of BNIP3L and BAK. Oncogene 2003;22:2172–85.

29. Walterhouse DO, Yoon JW, Iannaccone PM. Developmental pathways: Sonic hedgehog-Patched-GLI. Environ Health Perspect 1999;107:167–71.

30. Amin A, Li Y, Finkelstein R. Hedgehog activates the EGF receptor pathway during Drosophila head development. Development 1999;126:2623–30.

31. Dahmane N, Sanchez P, Gitton Y, et al. The Sonic hedgehog-Gli pathway regulates dorsal brain growth and tumorigenesis. Development 2001;128:5201–12.

32. Taipale J, Cooper MK, Maiti T, Beachy PA. Patched acts catalytically to suppress the activity of Smoothened. Nature 2002;418:892–7.

33. Murone M, Rosenthal A, de Sauvage FJ. Sonic hedgehog signaling by the patched-smoothened receptor complex. Curr Biol 1999;9:76–84.

34. Ruiz i Altaba A, Stecca B, Sanchez P. Hedgehog-Gli signaling in brain tumors: stem cells and paradevelopmental programs in cancer. Cancer Lett 2004;204:145–57.

35. Chuang PT, McMahon AP. Vertebrate Hedgehog signalling modulated by induction of a Hedgehog-binding protein. Nature 1999;397:617–21.

36. Pasca di Magliano M, Hebrok M. Hedgehog signalling in cancer formation and maintenance. Nat Rev Cancer 2003;3:903–11.

37. Berman DM, Karhadkar SS, Maitra A, et al. Widespread requirement for Hedgehog ligand stimulation in growth of digestive tract tumours. Nature 2003;425:846–51.

38. Vlahovic G, Crawford J. Activation of tyrosine kinases in cancer. Oncologist 2003;8:531–8.

39. Corless CL, Fletcher JA, Heinrich MC. Biology of gastrointestinal stromal tumors. J Clin Oncol 2004;22:3813–25.

40. Buchdunger E, Cioffi CL, Law N, et al. Abl protein-tyrosine kinase inhibitor STI571 inhibits *in vitro* signal transduction mediated by c-kit and platelet-derived growth factor receptors. J Pharmacol Exp Ther 2000;295:139–45.

41. Sjoblom T, Shimizu A, O'Brien KP, et al. Growth inhibition of dermatofibrosarcoma protuberans tumors by the platelet-derived growth factor receptor antagonist STI571 through induction of apoptosis. Cancer Res 2001;61:5778–83.